Journal of Science and Technology in Civil Engineering, HUCE (NUCE), 2022, 16 (4): 87–99

A NUMERICAL ANALYSIS ON BENDING CAPACITY OF STEEL PIPE COLUMNS USING A MECHANICAL JOINT WITH CONCRETE-FILLED STEEL TUBE

Nguyen Canh Tuan[a,b,*], Nguyen Thai Khiem[a,b]

[a]*Department of Bridge and Highway Engineering, Faculty of Civil Engineering, Ho Chi Minh City University of Technology (HCMUT), 268 Ly Thuong Kiet street, District 10, Ho Chi Minh City, Vietnam*
[b]*Vietnam National University Ho Chi Minh City (VNU-HCM), Linh Trung Ward, Thu Duc City, Ho Chi Minh City, Vietnam*

Article history:
Received 09/6/2022, Revised 25/8/2022, Accepted 26/8/2022

Abstract

Structural steel pipes have been applied commonly in the bridge construction for foundations or piers with many advantages such as large bending capacity, high shear resistance, and rapid construction. However, site welded joints may face critical technical matters which need to be considered for steel pipe piers during construction stage. Current solutions for pipe joints require the use of high-strength materials with machining technology to ensure accuracy, quality, and increase construction costs with substantial number of joints. Therefore, these solutions, when applied in Vietnam, will also face limitations due to the contractor's qualification and erection technology at construction site. This study proposes a type of joint for steel pipe piers of viaducts in a mountainous region to eliminate the welding work of the steel pipe at the construction site and to provide high bearing capacity, simple construction, and cost effectiveness. Finite element analyses are conducted to investigate and verify the bending capacity of steel pipes with the proposed joint. Nonlinear material and nonlinear geometry are considered to simulate behaviors of composite action, yielding, and buckling in the structures. Finally, comparative studies of bending capacity of the steel pipe with and without joint are performed. Stress distributions and deformations of the structural components in the joint region are also observed and discussed.

Keywords: bending capacity; steel pipe joint; concrete-filled steel tube; buckling; finite element analysis.

https://doi.org/10.31814/stce.nuce2022-16(4)-07

1. Introduction

Structural solutions using steel pipes have been applied commonly in the bridge construction for foundations or columns with many advantages such as large bending and shearing capacity, rapid construction. In Japan, steel pipes are majorly applied in construction of viaducts in mountainous regions [1] Such solution has brought outstanding efficiency compared to other types of structure under similar conditions. Fig. 1 shows a type of viaducts in the mountain using steel frame structures supported by steel pipe columns.

However, several technical matters need to be considered for steel pipe columns such as site welded joint of steel pipe during construction stage. The in-situ manufacture of the steel pipe joint cannot ensure the quality and affect the service durability of the structures. Some solutions for the

*Corresponding author. *E-mail address:* ctnguyen@hcmut.edu.vn (Tuan, N. C.)

Figure 1. A viaduct in mountainous region using steel pipe columns [2]

steel pipe joint based on the mechanical joint have been developed by JFE Steel Cooperation and Nippon Steel Corporation (Japan). These inventions have been patented and commercialized in many projects using steel pipe structure in Japan.

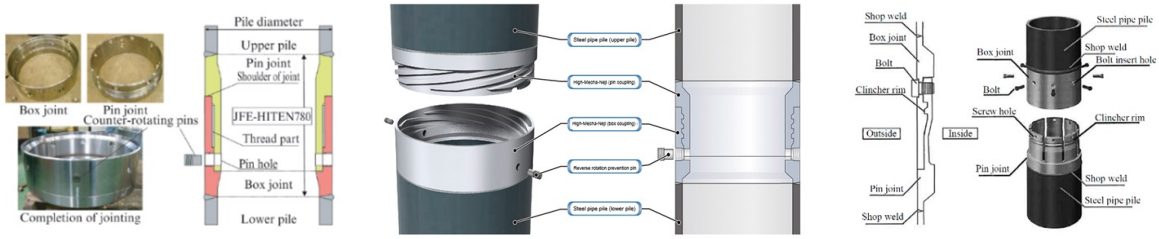

(a) Structure of "High-Mecha-Neji^{TM}" joint

(b) Design of "New High-Mecha-Neji" threaded joint

(c) Mechanical joint "KASHEEN"

Figure 2. Mechanical joint developed by JFE Steel Corporation (Japan) [3, 4]

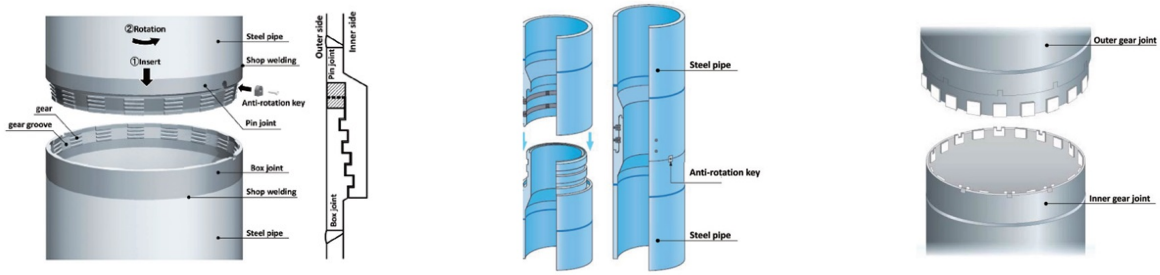

(a) Shape of "Gachi-cam" joint

(b) Joint and load transmission key "Laqnican"

(c) Joint with gear "Hi-SHJ"

Figure 3. Mechanical joint developed by Nippon Steel Corporation (Japan) [5]

The bearing mechanism of the “High-Mecha-Neji” threaded joint (Figs. 2(a) and 2(b)) is based on parallel bearing threads which are fabricated from the high strength steel (JFE-HITEN780) with a yield strength up to 685 Mpa and a tensile strength up to 780 Mpa. After being rolled and heat treated, threads are machined automatically. The thickness of the joint ring is limited due to high strength steel material. Therefore, such joint type is only applicable in several construction methods such as pile drilling and lowering, pile rotation, pile pressing with diameter from 318.5 mm to 1,200 mm. The study results also showed that the bearing capacity (bending, axial compression, axial tension, and shear) of the joint was larger than that of the steel pipe pile. To increase the efficiency and application range of the joint, authors have also improved the thread structure with larger-sized helical threads which can be applied in pile driving method. This improved joint is applicable to steel pipe piles up to 2,000 mm in diameter. The mechanical joint "KASHEEN"(Fig. 2(c)) was introduced by Akutagawa et al. in the technical report of JFE company [4]. The structure of the joint consists of yin-and-yang parts of welded to the steel pipe wall at the factory. The joint is fixed with pins using high strength bolts. The splice part is also fabricated from high strength steel (JFE-HITEN780). This joint is used for steel pipe piles with thick walls and diameters up to 1,600 mm which is applicable for most piling construction methods. Kitahama et al. [5] have also developed another mechanical joint using connecting mechanism with teeth and pins for fixing (Fig. 3). Joints are made of steel with a tensile strength up to 880 Mpa. The joint part will be welded to the steel pipe at the factory. Apllication range in diameters are from 400 mm to 1,600 mm with thicknesses from 6 mm to 30 mm.

Several mechanical joint solutions for steel pipe structures have also been developed by many other researchers. Uotinen and Tantala [6] have proposed a solution to connect steel pipe piles using threaded joints directly machined on the steel pipe piles which are applied in the pile driving method. The research results show that the bending resistance can reach only 75% maximum compared to the bending resistance of the pile body. The axial compressive resistance of the joint is also decreased because this joint type reduces the stability resistance of the steel pile body. This method also requires pre-fabricating the threaded line at the factory, and the pipe wall must be thick enough to be able to process the high-load thread type. Mechanical joints are also developed and applied in many practical projects for prestressed concrete piles (PHC) [7, 8]. Thus, current solutions for pipe joints require the use of high-strength materials with machining technology to ensure accuracy, quality, and increase construction costs with large number of joints. Therefore, these solutions, when applied in Vietnam, will also face many limitations due to the contractor’s qualification and erection technology at construction site.

This study proposes a type of joint for steel pipe columns of viaducts in a mountainous region using a composite structure with double-pipe mechanism. The mechanical joint will eliminate the welding work of the steel pipe at the construction site which provide high bearing capacity, simple construction, and cost effectiveness. The structure of the joint includes a connecting steel pipe segment with outer diameter, D_j, which is smaller than the inner diameter of the steel pipe, D, to ensure a small gap between the two pipes. The connecting steel pipe is strengthened with in-situ reinforced concrete. In addition, the anchor pin can be used to prevent slipping effect between the concrete core and the steel pipe and improve torsional resistance. The configuration of the composite steel pipe joint is shown in Fig. 4.

The bending capacity of the steel pipe joint is based on the mechanical behavior of the joint components. The steel joint pipe contributes the major bending strength by providing the continuous section of the steel pipe wall at the connection position. The thickness of the steel joint pipe will be calculated to ensure the stiffness of the joint. To increase the joint stiffness, the joint pipe is filled

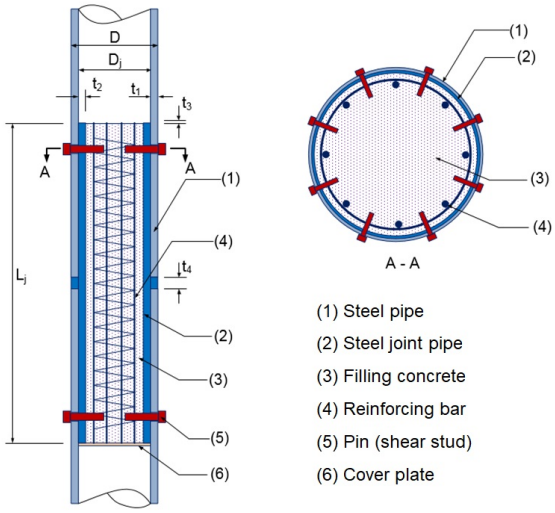

Figure 4. Structural composition of composite steel pipe joint

with reinforced concrete. Anchor pins will be provided at both ends of the joint to create the anchoring effect and improve torsional behavior of the joint.

The advantages of the proposed solution are to eliminate the site weld joint, easy to fabricate, and rapid to construct. Steel pipe columns can be loaded immediately after installation. The proposed solution is feasible and will reduce construction time and costs for viaducts in the mountainous regions. Finite element analyses are conducted to investigate and verify the bending capacity of the steel pipes with the proposed joint. Nonlinear material and nonlinear geometry are considered to provide accurate behaviors of composite action, yielding, and buckling in the structures. Finally, comparative studies of bending capacity of the steel pipe with and without joint are performed. Stress distributions and deformations of the structural components in the joint region are also observed and verified.

2. Simplified methods to calculate the bending strength of a composite steel pipe joint

2.1. Flexural resistance of composite steel pipe joint

The flexural resistance calculation theory of the concrete filled steel tube (CFST) has been successfully developed and provided in current bridge design specifications [9, 10]. Fig. 5 describes the Plastic Stress Distribution Method (PSDM) of the CFST with reinforcing steel bars.

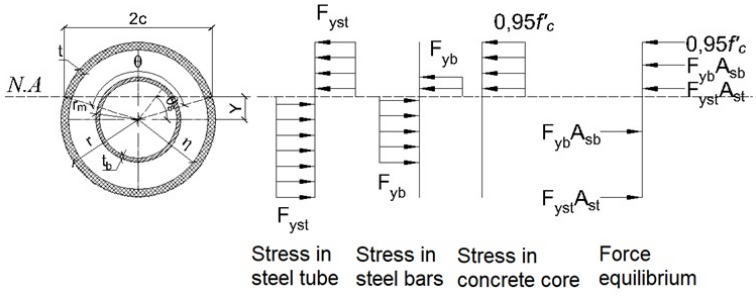

Figure 5. Plastic stress distribution model of a CFST

The composite steel pipe joint can be considered as a concrete-filled steel tube. Thus, the bending resistance of a CFST section is combined from the resistance of the concrete core, the reinforcing bar, and the steel tube. From the plastic stress distribution model, by neglecting the axial force, the bending capacity is determined by equilibrium condition of the external moment and internal moments by coupling plastic forces at the centroid of the structural components. The nominal bending resistance can be calculated as following equations:

$$M_n = 0.95 f_c' \left[\left(r_1^2 - y^2 \right) - \frac{c^2}{3} \right] + 4 F_{yst} t c \frac{r_m}{r_1} + 4 F_{yb} t_b c_b r_b \tag{1}$$

where

$$r_m = r - t/2; \quad \theta_b = \sin^{-1}(y/r_b); \quad c_b = r_b \cos\theta_b$$
$$\theta_s = \sin^{-1}(y/r_m); \quad c = r_i \cos\theta_s; \quad t_b = nA_b/2\pi r_b$$

in which A_b is area of a typical steel bar comprising the internal reinforcement (mm^2); c is one half the chord length of the tube in compression (mm); c_b is one half the chord length of a notional steel ring equivalent to the internal reinforcement in compression (mm); F_{yb} is yield stress of steel bar (Mpa); F_{yst} is yield stress of steel tube (Mpa); f_c' is compressive strength of concrete core (Mpa); n is number of internal steel reinforcing bars; r is radius to the outside of the steel tube (mm); r_b is radius to the center of the internal reinforcing bars; r_i is radius to the inside of the steel tube (mm); r_m is radius to the center of the steel tube (mm); t is wall thickness of the tube (mm); t_b is wall thickness of a notional steel ring equivalent to the internal reinforcement (mm); Y is distance from the center of the steel tube to the neutral axis (mm); θ_b is angle used to define c_b (rad), θ_b shall be taken as $\pi/2$ if y/r_b is greater than 1 and θ_b shall be taken as $-\pi/2$ if y/r_b is less than -1 (rad); θ_s is angle used to define c (rad).

2.2. Bending strength of a steel tube

The ultimate bending capacity of a hollow steel tube M_p was obtained using following equation [11]:

$$M_p = ZM_y = SZF_y \tag{2}$$

where Z is the elastic section modulus, $Z = \pi \left[d^4 - (d - 2t)^4 \right] / 32d$; d is the diameter of the steel pipe (mm); t is wall thickness (mm); F_y is the yield stress of steel pipe (Mpa); S is shape factor of the section, $S = 1.27$ for a circular tube.

3. Finite element analyses

3.1. Modelling method

To investigate the pure bending resistance of the proposed mechanical joint, a simply supported beam subjected to concentrated loads at two points is considered and simulated using a finite element method (FEM). The loading model is described in Fig. 6 with the boundary conditions and corresponding bending moment and shear diagrams. The figure shows the maximum moment region with the value $M_{\max}$ located between two loading points so that the joint must be placed within this region to fully received the pure bending property.

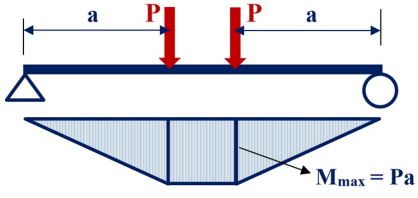

Figure 6. Loading model for a pure bending moment behavior

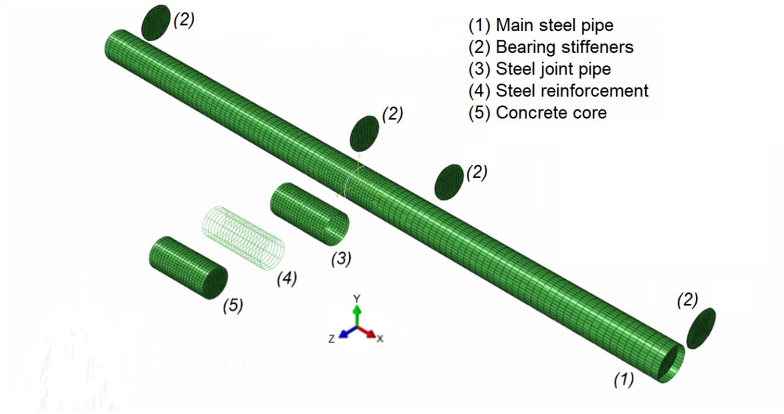

Figure 7. Structural components of a mechanical joint from a FEM model

The analyzed structural model contains two asymmetric steel pipes connected by a mechanical joint which includes the steel pipe joint and the reinforced concrete core. Fig. 7 shows components and configurations of the finite element model. Finite element models are conducted using an advanced structural analysis program ABAQUS [12]. The main steel pipe and the joint steel pipe are simulated using 4-node shell elements (S4R) while the concrete core is assigned as a general-purpose linear brick element (C3D8R) with 8 nodes. Steel bars and spirals reinforced inside the concrete core are simulated as truss elements (T3D2) which are embedded into the concrete core brick elements. Interactions between two main pipes (Fig. 8(a)), main pipes to joint pipe (Fig. 8(b)), and joint pipe (Fig. 8(c)) to concrete core are obtained by using GAP elements which can simulate bearing and friction behaviors. This type of element recreates the space between the interacted components and is only activated when the sliding friction movements or bearing contacts between components occur. Similar approach has been proposed and verified under various loading conditions by Moon et al. This study applies meshing method with 40 elements around the perimeter of the tube which satisfies mesh convergence proposed by Moon et al. for a concrete-filled steel tube section [13]. The GAP element allows separation of two nodes while it prevents pushing between the adjacent nodes. Thus,

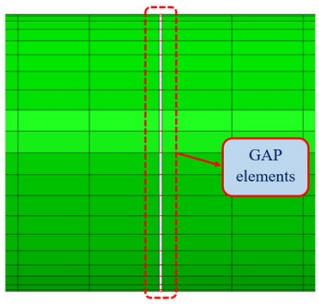

(a) Edge between pipes

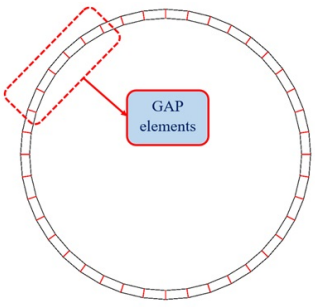

(b) Surfaces between pipes

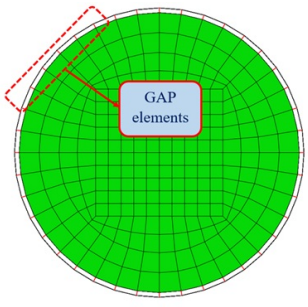

(c) Surfaces between pipe and concrete core

Figure 8. Bearing behaviors from friction interactions using GAP elements

the compression in the GAP element can be transferred as the confinement stress to the concrete core. Shear stress generated by friction sliding between nodes can be considered by assigning a friction coefficient to the GAP element. The initial distance between two nodes is set to zero to simulate the interface of the joint. The friction coefficients are 0.47 and 0.60 for gap elements between steel pipe and joint pipe and between joint pipe and concrete core have the friction, respectively. Cho et al. has also successfully conducted similar proposed finite element modelling methods to evaluate the flexural strength of the concrete-filled steel tube composite girder [14].

In the mechanical joint model, the material of the steel tubes and the reinforcement bars are assigned based on tri-linear stress-and-strain diagram illustrated in Fig. 9 and Fig. 10, with the same elastic modulus E_s = 200,000 Mpa. The steel pipes are assumed to have the yield strength at F_y = 345 Mpa and the tensile strength at F_u = 490 Mpa while yield strength of steel bars is F_y = 400 Mpa and the tensile strength is F_u = 570 Mpa.

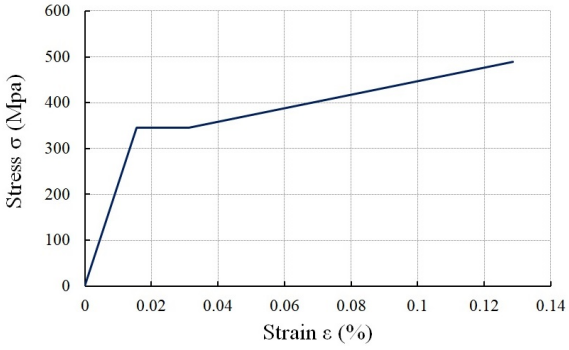

Figure 9. Stress-strain material model of steel pipes

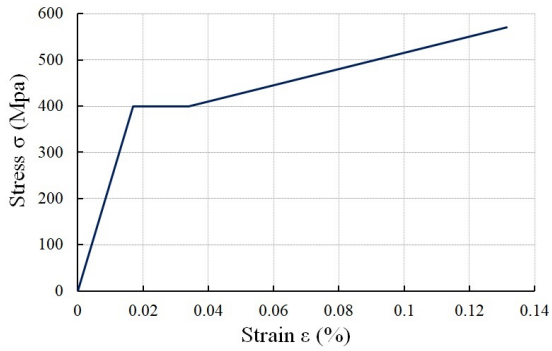

Figure 10. Stress-strain material model of reinforcement steel bars

Studies on the constitutive model of the concrete were successfully conducted. Lubliner et al. [15] developed a constitutive model based on an internal variable-formulation of plasticity theory for the non-linear analysis of concrete. A new plastic-damage model for concrete subjected to cyclic loading was proposed by Lee et al. [16] considering tensile damage and compressive damage. A yield function with multiple hardening variables were also introduced. Several recent studies have been also successfully applied the similar concrete model to simulate the composite structures such as concrete-filled tubular column [17, 18]. In this study, the concrete damaged plasticity model is considered using a theory developed by Hsu and Mo [19] that describes the behaviors of concrete under multiple stress states in both compression and tension. To assign the concrete material in the finite element model, the un-confined uniaxial compressive stress-strain curve was assumed as follows

$$f_c = f_c' \left\{ 2\frac{\varepsilon_c}{\varepsilon_c'} - \left(\frac{\varepsilon_c}{\varepsilon_c'}\right)^2 \right\} \tag{3}$$

where, f_c' is the compressive strength, and ε_c' is the strain corresponding to f_c' and was taken as 0.003. For the tensile behavior, the tension damage model is given as.

$$\begin{aligned} f_c &= E_c \varepsilon_c \\ f_c &= f_{cr}(\varepsilon_{cr}/\varepsilon_c)^{0.4} \end{aligned} \tag{4}$$

where, E_c is the Young's modulus of the concrete, f_{cr} is the cracking stress of the concrete, and ε_{cr} is the cracking strain of the concrete. For the finite element model, the dilation angle at 20 degrees were

used for the concrete core based on the results of a previous study [14]. The uni-axial stress–strain relationship is shown in Fig. 11. In this concrete model, the compression strength is defined as $f_c^{'}$ = 28 Mpa and the tensile strength of the concrete is taken as f_{cr} = 2 Mpa.

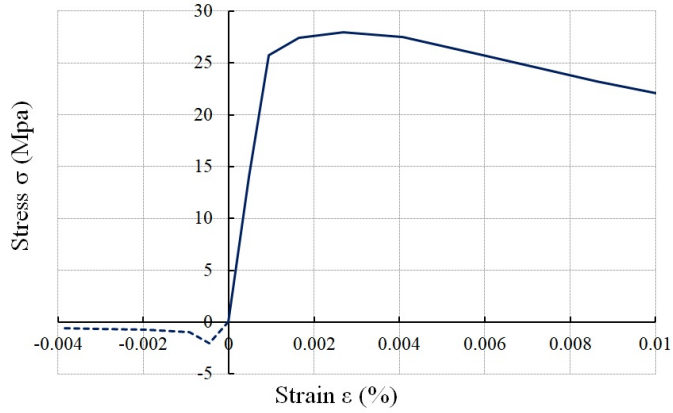

Figure 11. Stress-strain material model of concrete

Twelve finite element models are conducted to investigate the bending capacity of the steel pipe with and without joints. The diameters vary from 200 mm to 500 mm, and corresponding lengths are taken as $10D$ + 200 mm. With each diameter, four distinctive specimens representing cases of steel pipes without joint (M0), steel joint pipe with reinforced concrete (M1), steel joint pipe with bared concrete core (M2), and steel pipe joint using only (M3). The ratio between effective lengths and diameters of analysis model is fixed so that bending behaviors are easy to observe and the convergence

Table 1. Profiles of conducted finite element models

Model		Steel main pipe			Steel joint pipe		
		D	t	L_i	D_j	t_j	L_j
		(mm)	(mm)	(mm)	(mm)	(mm)	(mm)
D200	M0	200	6	2,100	-	-	-
	M1				188	6	1,000
	M2				188	6	1,000
	M3				188	6	1,000
D350	M0	350	8	3,600	-	-	-
	M1				334	8	1,000
	M2				334	8	1,000
	M3				334	8	1,000
D500	M0	500	8	5,100	-	-	-
	M1				484	8	1,000
	M2				484	8	1,000
	M3				484	8	1,000

of nonlinear analyses can be obtained. The joint length is fixed at L_j = 1,000 mm considering actual fabrication and installation of joint components. Therefore, effects of length ratios between the length of main pipes and joints can be investigated. Profiles of all analysis models are shown in Table 1.

The alignment of the analysis model of two main pipes with a mechanical joint is illustrated in Fig. 12. Loading positions are located at a distance 500 mm from edges of the pipe joint. The beam model is simply supported with a pinned end and a roller end located 100 mm from each end. To prevent local buckling and yielding of steel pipe at supports and loading positions, strong stiffeners with 20 mm thickness are applied. To secure the pure in-plan bending behavior, the steel pipe is restrained vertically at each end stiffener to prevent rotation about axis and lateral displacement in direction of supports (see Fig. 13). The model is loaded to reach the ultimate bending strength. To generate applied loads, forced displacements are assigned at loading points, and the magnitude of the equivalent applied forces is measured from the reaction forces at the loading points.

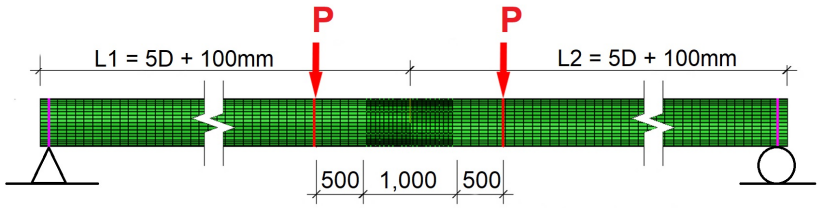

Figure 12. Loading plan and boundary condition model for analysis

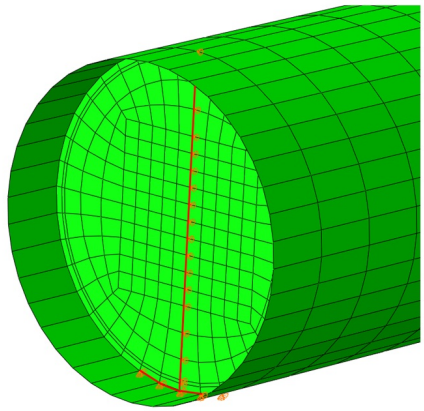

Figure 13. Lateral and torsional restraints at a bearing stiffener

3.2. Analysis results and verifications

To verify the bending capacity of the steel pipe joint in comparison to the steel pipe without joint, equivalent critical bending moments from all finite element analyses are calculated from the peak loading reactions. The critical bending moments are then compared with theoretical plastic bending moment of the steel main pipe with no joint. Table 2 shows the comparative studies of bending capacities between the theoretical study and finite element analyses. The theoretical values of bending moment are calculated based on the Eq. (2) for the steel pipe without joint. The critical bending moment can be defined as the maximum bending moment at a corresponding peak loading value. The

equivalent critical bending moment can be also defined using Southwell-Plot method [20] in case peak loading value cannot be clearly found. From the results, the critical bending moments of the M0 models from FEM analyses are well matched with those from theory with maximum difference at 2.0%. The results also reveal that the proposed pipe joint provide sufficient strength to ensure the continuous rigidity along the steel pipe under bending. Results from Table 2 also show that pipe joints significantly contribute additional bending capacity to the total strength of steel pipes especially for the cases of infilled concrete. The bending capacity of steel pipes with joints are larger than that of steel pipes without joint from 4.8% to 21.6%. The bending strengths of the steel pipes without joints are almost consistent with those from the theory with maximum discrepancy at 2%.

Table 2. Comparative results of bending capacity of main steel pipes

Model		M_p [(Eq. (2))] (kNm)	M_{cr} [FEM] (kNm)	Difference (%)
D200 × 6	M0	75.4	74.0	1.9%
	M1		83.0	10.0%
	M2		82.9	9.8%
	M3		81.9	8.6%
D350 × 8	M0	314.8	317.5	0.8%
	M1		382.8	21.6%
	M2		356.5	13.2%
	M3		337.0	7.0%
D500 × 8	M0	655.9	642.9	2.0%
	M1		687.3	4.8%
	M2		687.2	4.8%
	M3		620.5	5.4%

To investigate the pure bending behavior, both bending moments and rotation angles are determined and plotted. From finite element analysis result, the equivalent rotation displacement θ_i around z axis at the support can be transformed from the vertical displacement at the loading points. The average rotation at supports is approximated as $\theta_i = \text{atan}\,(\delta/5D)$, where δ is the deflection at the bottom

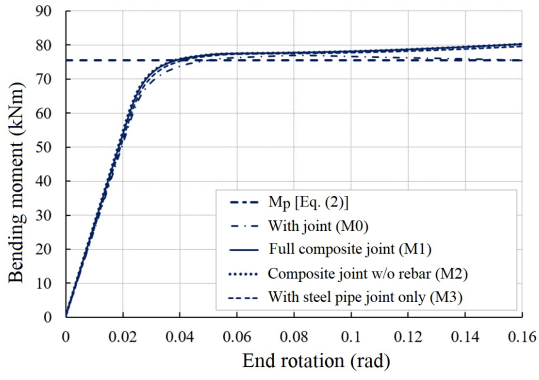

Figure 14. Comparison of bending capacity of pipe joints with D = 200 mm

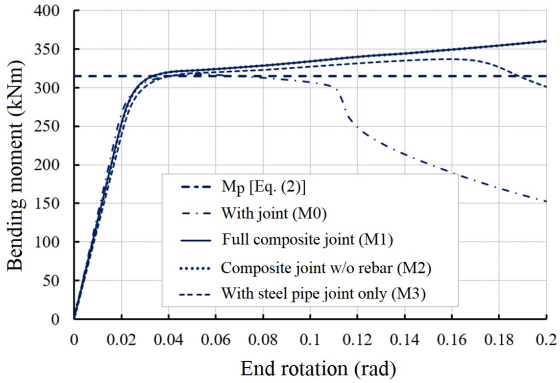

Figure 15. Comparison of bending capacity of pipe joints with D = 350 mm

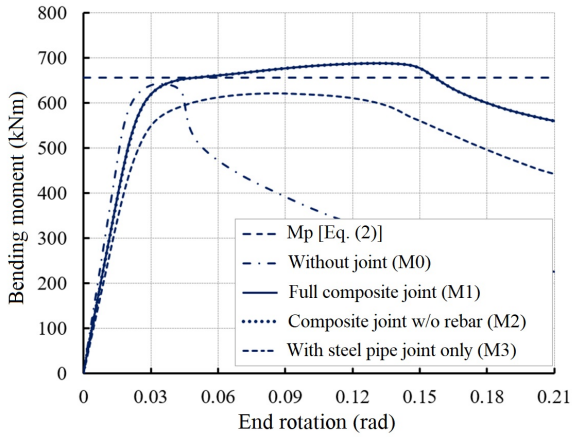

Figure 16. Comparison of bending capacity of pipe joints with D = 500 mm

fiber at the loading location (mm) and D is the diameter of the main pipe (mm). Figs. 14, 15 and 16 show the comparison of bending capacity of steel pipes with diameter D = 200 mm, D = 350 mm, and D = 500 mm respectively.

For the case D = 200 mm and the thickness t = 6 mm, the slenderness of the pipe section is small, so the bending capacity can reach the plastic bending moment without any local buckling. Stresses in the regions near edges of the pipe joints are much larger than those inside the joints. With the case D = 350 mm and t = 8 mm, the plastic bending moment can be achieved without any local buckling deformation. The yield stress almost develops in the whole section before failure due to large deformation and yielding at the loading regions. Fig. 17 shows the stress distributions at the joints of the model D200 and D350.

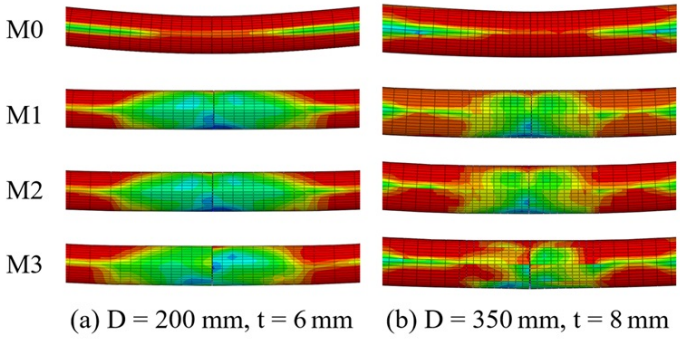

Figure 17. Stress distributions at the joints and loading locations

With the case D = 500 mm and t = 8 mm, the section slenderness is larger than those of other case. The yielding cannot develop in the whole section due to minor local bucking occurs in the compression fiber of the steel pipe. In this case, the critical bending moment of the main pipe with only steel joint pipe is smaller than that of the steel pipe without joint. Buckling behaviors in the joint pipe mitigates stiffness of the joint and increase deformation at the joint edge. The results also reveals that the concrete core effectively contributes more bearing stiffness to the joint rigidity. Figs. 18 and 19 show the failure deformation due to local buckling at the joint and the stress distribution inside the

concrete core. At the failure mode, the buckling deformation occurs at the midpoint of the steel pipe without joint while the pipe joints with concrete core and rebars tend to be destructed at the edge of the joints. Fig. 19 shows propagation paths of the compression tress in the concrete cores, which are similar to strut-and-tie models.

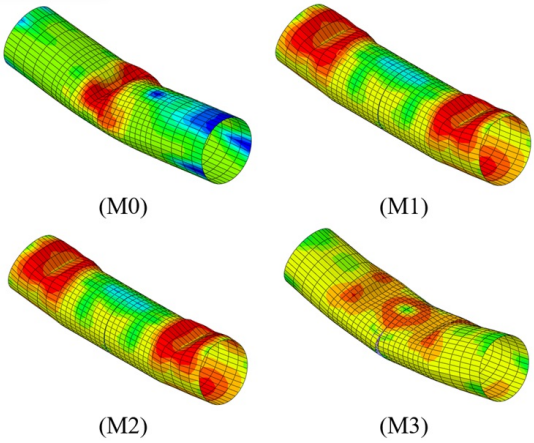

Figure 18. Buckling deformations and stress distribution at pipe joints (D500)

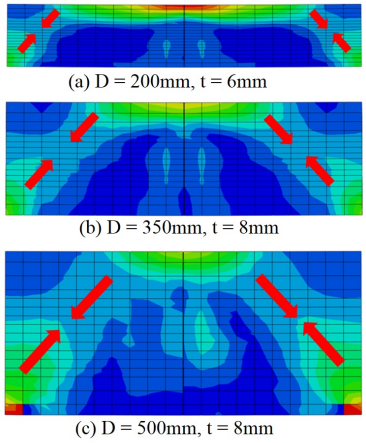

Figure 19. Stress distributions inside concrete core of the composite pipe joints

4. Conclusions

This research proposes a structural solution for the steel pipe connection using a mechanical joint with a composite steel pipe. Several finite element models have been conducted to investigate and verify the bending capacity of the proposed steel pipe joints. For finite element analyses, nonlinear material and large deformation have been considered to simulate actual bending behaviors of the structure. Comparative studies of the bending capacities between steel pipes without joint and steel pipes with joints have been performed. Results have shown that the proposed steel pipe joints have provided sufficient bending capacity in comparison to pipes without joint. The effects of reinforced concrete core on the joint stiffness are also observed. It is revealed that the core has contributed more rigidity to the joint which prevents local buckling deformation so that the maximum bending capacity can be achieved. In order to improve the stability of the pipe wall under bending, the slenderness of the pipe wall which is represented by the ratio between the diameter and the thickness should be considered.

The results have shown that the proposed composite pipe joints are effective and feasible to apply in actual viaduct structures. For further research, practical experiments should be conducted to confirm the effectiveness of the proposed solution. In addition, effects of torsion and axial force should be considered to simulate actual behaviors of steel pipe columns as vertical support members in viaduct structure.

Acknowledgements

The research is funded by Ho Chi Minh City University of Technology – Viet Nam National University Ho Chi Minh City under grant number To-KTXD-2021-18. We acknowledge Ho Chi Minh City University of Technology (HCMUT), VNU-HCM for supporting this study.

References

[1] Kobayashi, H., Yonezawa, H., Hiwatashi, K., Nakaji, T. (2005). "Metal Road" Method - Diversification of Coverage and High Resistivity against Natural Disaster. *JFE Technical Report*, (10):16–25.

[2] Metal Road Construction Method Association (2009). *Metal Road Method - Design and construction manual*. Japan.

[3] Ichikawa, K., Sato, R., Terao, N. (2020). Development of Mechanical Joint New "High-Mecha-Neji" for Steel Pipe Piles and Steel Pipe Sheet Piles. *JFE Technical Report*, (25):9–16.

[4] Akutagawa, H., Takano, K., Tajika, H. (2006). Mechanical Joint "KASHEEN" for Large-Diameter Pipe Piles. *JFE Technical Report*, (8):51–56.

[5] Masashi, K., Yoshiro, I., Hironobu, M., Yoshinori, F., Toshihiko, S., Shinji, T., Tadachika, M., Hiroyuki, T. (2016). Development of the Mechanical "Gachi-cam Joint" for Steel Pipe Piles and Steel Pipe Sheet Piles. *Nippon Steel & Sumitomo Metal Technical Report*, (113):34–41.

[6] Veli-Matti, U., Jukka, R. (2013). Applications and Development of Modern Steel Pile Technology. In *Proceeding 11th International Conference on Modern Building Materials, Structures and Techniques, MBMST*, 1173–1182.

[7] Shin, Y., Kim, M., Ko, J., Jeong, S. (2013). Proposed design chart of mechanical joints on steel-PHC composite piles. *Materials and Structures*, 47(7):1221–1238.

[8] Hu, H., Zhao, F., Tang, M., Zhang, S., Chen, H. (2018). The design and optimization of an emerging pile coupling with application to drilled and PHC pipe cased piles. *IOP Conference Series: Materials Science and Engineering*, 423:012028.

[9] TCVN 11823:2017. *Highway Bridge Design Specification*. Ha Noi, Vietnam.

[10] AASHTO (2020). *LRFD Bridge Design Specification*. The American Association of State Highway and Transportation Officials, Washington DC, USA.

[11] Wong, M. B. (2009). *Plastic analysis and design of steel structures*. Burlington (MA), Butterworth.

[12] ABAQUS (2017). *Standard User's Manual Version 6.13*. Hibbit, Karson and Sorensen Inc.

[13] Moon, J., Roeder, C. W., Lehman, D. E., Lee, H.-E. (2012). Analytical modeling of bending of circular concrete-filled steel tubes. *Engineering Structures*, 42:349–361.

[14] Cho, J., Moon, J., Ko, H.-J., Lee, H.-E. (2018). Flexural strength evaluation of concrete-filled steel tube (CFST) composite girder. *Journal of Constructional Steel Research*, 151:12–24.

[15] Lubliner, J., Oliver, J., Oller, S., Oñate, E. (1989). A plastic-damage model for concrete. *International Journal of Solids and Structures*, 25(3):299–326.

[16] Lee, J., Fenves, G. L. (1998). Plastic-Damage Model for Cyclic Loading of Concrete Structures. *Journal of Engineering Mechanics*, 124(8):892–900.

[17] Phan, H. D. (2021). Numerical analysis of seismic behavior of square concrete filled steel tubular columns. *Journal of Science and Technology in Civil Engineering (STCE) - HUCE*, 15(2):127–140.

[18] Son, T., Ngo-Huu, C., Thuat, D. V. (2021). Finite element modelling of rectangular concrete-filled steel tube stub columns incorporating high strength and ultra-high strength materials under concentric axial compression. *Journal of Science and Technology in Civil Engineering (STCE) - HUCE*, 15(4):74–87.

[19] Hsu, T. T. C., Mo, Y. L. (2010). *Unified Theory of Concrete Structures*. Wiley.

[20] Luis A., G. (1999). *Theory of Elastic Stability: Analysis and Sensitivity*. 1st edition, CRC Press.